doi:10.1093/brain/awq047 Brain 2010: 133; 1094–1110 | 1094

BRAIN
A JOURNAL OF NEUROLOGY

Cell loss in the motor and cingulate cortex correlates with symptomatology in Huntington's disease

Doris C. V. Thu,[1,2,3] Dorothy E. Oorschot,[4] Lynette J. Tippett,[2,5] Alissa L. Nana,[1,2] Virginia M. Hogg,[2,5] Beth J. Synek,[2,6] Ruth Luthi-Carter,[3] Henry J. Waldvogel[1,2] and Richard L. M. Faull[1,2]

1 Department of Anatomy with Radiology, University of Auckland, Private Bag 92019, Auckland, New Zealand
2 Centre for Brain Research, University of Auckland, Private Bag 92019, Auckland, New Zealand
3 Brain Mind Institute, École Polytechnique Fédérale de Lausanne (EPFL), Lausanne, Switzerland
4 Department of Anatomy and Structural Biology, Otago School of Medical Sciences, University of Otago, New Zealand
5 Department of Psychology, University of Auckland, Private Bag 92019, Auckland, New Zealand
6 Department of Forensic Pathology, Auckland City Hospital, Auckland, New Zealand

Correspondence to: Professor Richard L. M. Faull,
Centre for Brain Research,
Faculty of Medical and Health Sciences,
University of Auckland, Private Bag 92019,
Auckland, New Zealand
E-mail: rlm.faull@auckland.ac.nz

Huntington's disease is an autosomal dominant inherited neurodegenerative disease with motor symptoms that are variably co-expressed with mood and cognitive symptoms, and in which variable neuronal degeneration is also observed in the basal ganglia and the cerebral cortex. We have recently shown that the variable symptomatology in Huntington's disease correlates with the variable compartmental pattern of $GABA_A$ receptor and cell loss in the striatum. To determine whether the phenotypic variability in Huntington's disease is also related to variable neuronal degeneration in the cerebral cortex, we undertook a double-blind study using unbiased stereological cell counting methods to determine the pattern of cell loss in the primary motor and anterior cingulate cortices in the brains of 12 cases of Huntington's disease and 15 controls, and collected detailed data on the clinical symptomatology of the patients with Huntington's disease from family members and clinical records. The results showed a significant association between: (i) pronounced motor dysfunction and cell loss in the primary motor cortex; and (ii) major mood symptomatology and cell loss in the anterior cingulate cortex. This association held for both total neuronal loss (neuronal N staining) and pyramidal cell loss (SMI32 staining), and also correlated with marked dystrophic changes in the remaining cortical neurons. There was also an association between cortical cell loss and striatal neuropathological grade, but no significant association with CAG repeat length in the Huntington's disease gene. These findings suggest that the heterogeneity in clinical symptomatology that characterizes Huntington's disease is associated with variation in the extent of cell loss in the corresponding functional regions of the cerebral cortex whereby motor dysfunction correlates with primary motor cortex cell loss and mood symptomatology is associated with cell loss in the cingulate cortex.

Received December 17, 2009. Revised January 20, 2010. Accepted February 2, 2010

Keywords: Huntington's disease; cingulate cortex; motor cortex; symptoms; stereology
Abbreviations: NeuN = neuronal N; N_v = numerical density; V_{ref} = reference volume

Introduction

Huntington's disease is an autosomal dominant neurodegenerative disease caused by a CAG expansion in the *HD* gene *(IT15)* on the short arm of chromosome 4 (The Huntington's Disease Collaborative Research Group, 1993). The disease results in neurodegeneration, principally in the basal ganglia and cerebral cortex of the forebrain (Vonsattel *et al.*, 1997), and is characterized by involuntary choreiform movements, as well as mood, cognitive and behavioural symptoms (Vonsattel *et al.*, 1997; Vonsattel and DiFiglia, 1998). Despite the single gene aetiology of Huntington's disease there is considerable phenotypic variation between cases in the pattern of symptomatology during the course of the disease. Some patients show mainly motor symptomatology at clinical onset and minimal dysfunction of either mood or cognition; while at the other extreme, others show mainly mood and/or cognitive changes, with minimal movement dysfunction until the late stages of the disease. In addition, others show a variable mixed phenotype of motor, mood and cognitive symptoms throughout the course of the disease (Brandt and Butters, 1986; Folstein, 1989; Myers *et al.*, 1991; Claes *et al.*, 1995; Zappacosta *et al.*, 1996; Thompson *et al.*, 2002). Although the number of CAG repeats in the Huntington's disease gene is negatively correlated with the age of symptom onset (Wexler *et al.*, 2004), there is no clear correlation between the variable symptom profile and CAG repeat number. Indeed, this lack of correlation between clinical phenotype and Huntington's disease genotype has been clearly demonstrated for monozygotic twins, who showed marked differences in symptom profile despite the inheritance of identical Huntington's disease genes (Georgiou *et al.*, 1999; Gomez-Esteban *et al.*, 2007).

The major neuronal degeneration in Huntington's disease occurs in the striatum of the basal ganglia and in the neocortex (Vonsattel *et al.*, 1997). Although Huntington's disease is characterized by an extensive degeneration of the GABAergic output neurons of the striatum (Reiner *et al.*, 1988; Vonsattel and DiFiglia, 1998; Deng *et al.*, 2004), there is considerable variation between Huntington's disease cases in the pattern of neurodegeneration between the two major compartments of the striatum—the striosome and matrix (Tippett *et al.*, 2007). Some cases show selective loss of striatal neurons and neurochemical markers in the striosomes (Morton *et al.*, 1993; Hedreen and Folstein, 1995; Augood *et al.*, 1996), while others show selective changes in the matrix (Olsen *et al.*, 1986; Ferrante *et al.*, 1987; Seto-Oshima *et al.*, 1988; Faull *et al.*, 1993), and yet other cases show dual compartmental degeneration (Tippett *et al.*, 2007). Since the differential pattern of connectivity of the striosome and matrix compartments in the mammalian brain suggest that the striosomes may play a role in limbic (e.g. mood) related functions, and the matrix compartment may contribute to motor functions, we recently investigated whether the differential compartmental pattern of striatal degeneration correlated with the variable symptomatology in Huntington's disease cases. In our study of 35 Huntington's disease cases (Tippett *et al.*, 2007), we showed a significant association between pronounced mood dysfunction and $GABA_A$ receptor and cell loss in the striosomes, suggesting that part of the variation in clinical symptomatology in Huntington's disease correlates with the variable pattern of compartmental neurodegeneration in the striatum.

In the present study, we have now extended our findings to determine whether the pattern of neurodegeneration in the cerebral cortex, the other major forebrain region known to be affected in Huntington's disease, also shows an association with symptom profile. Previous quantitative cell studies have established that widespread regions of the cerebral cortex are affected in Huntington's disease (Cudkowicz and Kowall, 1990; Hedreen *et al.*, 1991; Heinsen *et al.*, 1994; Macdonald *et al.*, 1997; Macdonald and Halliday, 2002; Selemon *et al.*, 2004). Major losses of pyramidal projection neurons have been documented for cases of Huntington's disease in various regions of the cerebral cortex including the motor cortex (Macdonald and Halliday, 2002), superior frontal cortex, cingulate gyrus (Cudkowicz and Kowall, 1990) and the angular gyrus of the parietal lobe (Macdonald *et al.*, 1997). These findings of cortical degeneration have been more recently extended in studies using high resolution *in vivo* magnetic resonance imaging and automated surface reconstruction to measure cortical thickness (Rosas *et al.*, 2002, 2003, 2004, 2005). These *in vivo* studies in over 30 individuals with Huntington's disease have elegantly shown a heterogeneous pattern of region-specific thinning of the cerebral cortex in Huntington's disease with some of the most marked changes being in the sensorimotor cortex and areas of the visual cortex (Rosas *et al.*, 2002, 2008). Distinct motor phenotypes were shown to be associated with discrete patterns of cortical thinning, whereas caudate volumes failed to discriminate the two clinical phenotypes. Rosas *et al.* (2008) concluded that cortical changes begin early in Huntington's disease, are regionally heterogeneous and that topologically selective changes in the cerebral cortex might explain much of the clinical heterogeneity found in Huntington's disease.

In the present study, we first tested the hypothesis that there is a loss of neurons in the primary motor cortex and the anterior cingulate cortex in 12 Huntington's disease brains compared to 15 control brains for our specific cohort of brains from the Neurological Foundation of New Zealand Human Brain Bank. We then tested the hypothesis that there is heterogeneity in cortical cell loss in Huntington's disease and that this heterogeneity correlates with symptomatology in a double-blind study of the

12 Huntington's disease cases. We used unbiased stereological cell counting methods to determine the pattern of total and pyramidal cell loss found post-mortem in the primary motor cortex and the anterior cingulate cortex. These are two functionally diverse regions of the cerebral cortex: the primary motor cortex is known to be involved in the control of motor functions, whilst the anterior cingulate cortex is involved in emotional regulation and mood disturbances (Ebert and Ebmeier, 1996; Davidson *et al.*, 2002; Harrison, 2002; Alexopoulos *et al.*, 2008; Konarski *et al.*, 2008). We then compared the pattern of cortical cell loss in the Huntington's disease cases with the pattern of motor and mood symptoms present during the disease for each case, as determined by retrospective analysis of clinical symptom data collected from patients, family members and clinical records. Our findings show that the heterogeneity in the motor and mood clinical symptomatology in Huntington's disease correlates with the heterogeneity of cell loss in the corresponding functional regions of the cerebral cortex and suggest that the pattern of cortical pathology contributes to the variability in behavioural symptomatology in Huntington's disease.

Materials and methods

All protocols used in this study were approved by the University of Auckland Human Participants Ethics Committee and informed consent was obtained from all families.

Neuroanatomical studies

Brain tissue from 12 cases of Huntington's disease (Table 1) and 15 controls (Table 2) was obtained from the Neurological Foundation of New Zealand Human Brain Bank. The cases of Huntington's disease included six males and six females, aged 35–75 years (average 61 years), with a post-mortem interval prior to perfusion between 3 and 24 h (average 14 h). The control cases included 10 males and five females with no history of neurological disease, aged 46–79 years (average 64 years), with a post-mortem interval between 5 and 21 h (average 12 h).

Brains were perfused as described previously (Waldvogel *et al.*, 2006) through the basilar and internal carotid arteries, first with phosphate buffered saline with 1% sodium nitrite, followed by 15% of formalin in 0.1 M phosphate buffer (pH 7.4) for 1 h. Following

Table 1 Huntington's disease cases

Case number	Gender	Age at death	CAG repeat length *HD* gene	Post-mortem delay (hours)	Grade	Symptoms	Cause of death
HC 60	Male	64	18/43	23	3	Mixed	Pneumonia
HC 68	Female	65	17/42	11	1	Motor	Cardiac arrest
HC 72	Female	63	17/42	24	2	Motor	Pneumonia
HC 73	Male	47	19/49	4	2	Motor	Pneumonia
HC 79	Female	56	17/42	4	1	Mixed	Cardio-respiratory failure
HC 82	Male	74	15/42	16	2	Mood	Pneumonia
HC 85	Female	61	24/44	19	3	Mood	Huntington's disease
HC 93	Female	56	20/43	17	3	Mixed	Pneumonia
HC 95	Female	66	20/39	12	2	Mood	Huntington's disease
HC 99	Male	68	21/41	13	2	Motor	Broncho-pneumonia
HC 101	Male	35	17/44	24	1	Mood	Asphyxia
HC 107	Male	75	19/43	3	3	Mixed	Broncho-pneumonia

Table 2 Control cases

Case number	Gender	Age of death	CAG repeat length	Post-mortem delay (hours)	Cause of death
H 108	Male	58	15/17	16	Coronary atherosclerosis
H 110	Female	83	17/17	14	Ruptured aortic aneurysm
H 111	Male	46	17/20	10	Coronary artery disease
H 112	Male	79	14/15	8	Bleeding stomach ulcer
H 115	Male	61	17/19	12	Hypertensive heart disease
H 118	Male	57	15/16	10	Coronary artery disease
H 120	Male	62	18/22	11	Ischaemic heart disease
H 121	Female	64	18/23	5	Pulmonary embolism
H 127	Female	59	15/17	21	Pulmonary embolism
H 129	Male	48	20/21	12	Pulmonary embolism
H 131	Female	73	17/17	13	Ischaemic heart disease
H 132	Female	63	15/19	12	Ruptured aorta
H 136	Male	75	N/A	13	Ruptured abdominal aortic aneurysm
H 139	Male	73	N/A	5.5	Ischaemic heart disease
H 330	Male	66	15/15	13	Cor pulmonale

perfusion, blocks (0.75–1.5 cm) were taken from the primary motor cortex and the anterior cingulate cortex of the right hemisphere and kept in the same fixative for 24 h. The blocks from the primary motor cortex were carefully selected from just above the mid dorsoventral region of the precentral gyrus, i.e. the portion corresponding topographically to cortical areas of the upper limb (Fig. 1A). The blocks from the cingulate gyrus were taken from the region of the anterior cingulate cortex immediately dorsal to the genu of the corpus callosum (Fig. 1B). The blocks were then cryoprotected in 20% sucrose in 0.1 M phosphate buffer with 0.1% sodium–azide for 2–3 days and in 30% sucrose in 0.1 M phosphate buffer with 0.1% sodium-azide for a further 2–3 days, then stored at –80°C until further processing.

Blocks were also taken from the basal ganglia for pathological examination. The neuropathologic 'striatal' grading of the Huntington's disease cases was undertaken according to the Vonsattel grading criteria (Grades 0–4) (Vonsattel *et al.*, 1985; Vonsattel and DiFiglia, 1998) by a neuropathologist (B.J.S.) with extensive experience in Huntington's disease neuropathology. On pathological examination, the control cases showed no neuropathological abnormalities.

For immunohistochemistry each cortical block was sectioned at 50 μm on a freezing microtome and the sections were processed free-floating in six-well tissue culture plates. Two random systematic series of sections were sampled from each entire tissue block from the motor cortex and cingulate cortex for each brain. Each series of sections were washed (3 × 15 min) in phosphate buffered saline and 0.2% Triton-X (phosphate buffered saline-triton), incubated for 20 min in 50% methanol and 1% H_2O_2, washed, and incubated in primary antibody for 3 days on a shaker at 4°C. The primary antibodies used were mouse anti-neuronal N (NeuN; Chemicon, 1:1000) to immunostain the total population of neurons and mouse anti-SMI32 (Sternberger Monoclonals Incorporated, 1:1000), against the non-phosphorylated epitopes in neurofilaments, to immunostain a subpopulation of pyramidal neurons. Sections that were stained with SMI32 underwent antigen retrieval treatment as described previously (Waldvogel *et al.*, 2006). Sections from both series were washed, incubated overnight in biotinylated goat anti-mouse secondary antibody (Sigma, 1:500), washed, incubated for 4 h at room temperature in ExtrAvidin™ (Sigma, 1:1000), washed, then exposed to 0.05% 3,3-diaminobenzidine tetrahydrochloride (Sigma) and 0.01% H_2O_2 for 15–20 min to produce a brown reaction product. The sections were washed, mounted on gelatine–chrome–alum coated slides, dried, dehydrated through a graded alcohol series to xylene and coverslipped with Hystomount (Hughes and Hughes, UK). Sections processed to determine non-specific staining by following the same immunohistochemical procedures, but with omission of the primary antibody, showed no immunohistochemical labelling. Before the stereological analyses all sections were coded and blinded.

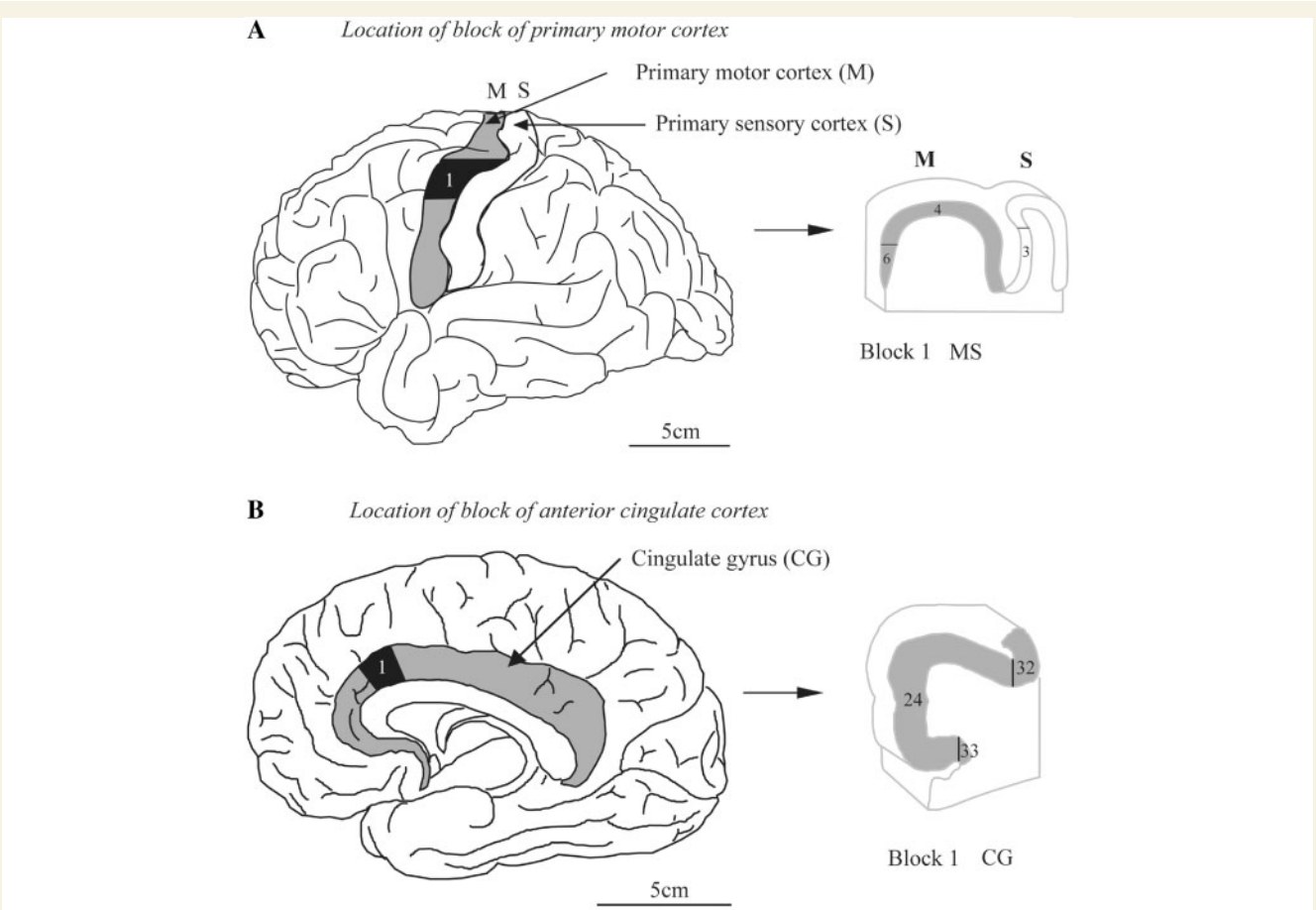

Figure 1 Diagram showing the location of each cortical block (indicated at 1) that was used for stereological analysis (**A**) in the primary motor cortex and (**B**) in the anterior cingulate cortex. Each cross-section of a block indicates the specific Brodmann cytoarchitectural region.

Stereology

In this study, a block (0.75–1.5 cm) of tissue in a well defined subregion of either the primary motor cortex (Fig. 1A) or the anterior cingulate cortex (Fig. 1B) was completely serially sectioned for subsequent stereological analyses. The absolute number of neurons within all of the primary motor cortex (i.e. all of Brodmann area 4) and all of the anterior cingulate cortex (Brodmann area 24) could not be measured because of a lack of tissue availability. While this approach is not stereologically optimal (Oorschot, 1994), an assumption was made that analysis of a quarter to a tenth of each of these cortical regions would yield data that were representative of each entire cortical region. For the primary motor cortex, the observed results were compared with previously reported control and Huntington's disease data on the absolute number of neurons within the entire primary cortex (i.e. all of Brodmann area 4, Macdonald and Halliday, 2002; see Results and Discussion sections). For the cingulate cortex, the observed results were compared with previously reported control and Huntington's disease data on the number of neurons per length of cerebral cortex for Brodmann area 24 (Cudkowicz and Kowall, 1990).

The total number of neurons (N) within a defined volume of Brodmann area 4 in the primary motor cortex (Fig. 1A), and within a defined volume of Brodmann area 24 in the anterior cingulate cortex (Fig. 1B), was derived from random systematically sampled sections of each cortical block. The total reference volume (V_{ref}) of each block or defined region was multiplied by the number of neurons in a defined subvolume of each central region (N_v). Thus, $N = V_{ref} \times N_v$.

The total reference volume of each region of interest was determined by using Cavalieri's direct volume estimate (Gundersen and Jensen, 1987). This was obtained by estimating the cross-sectional area of each region of interest in 10 systematically sampled sections throughout the defined volume of interest and multiplying the sum of the area of the 10 sections by the distance between each sampled section. The cross-sectional area of each section was estimated using a point-counting method. Each sampled section was projected onto a colour monitor at a known magnification and a lattice of regularly arranged points was superimposed on it. The number of points falling on the region of interest was counted (ΣP) and the total volume was determined using the formula: $V_{ref} = \Sigma P \cdot a(p) \cdot t \cdot 10$, where $a(p)$ is the real area that each point represents, t is the average thickness of the sections and '10' is the distance between the sampled sections. The real interpoint distance and real $a(p)$ of a lattice used for each cortical region are listed in Table 3.

The numerical density (N_v) within each cortical region was estimated by using the optical disector method. The sections used for each region were the same set of sections that were used for Cavalieri's estimate of volume (V_{ref}) above. Each sampled section was viewed using a 100 × oil immersion objective. The microscope was equipped with a microcator on the focus control (to measure the z-axis), an automated mechanical stage and a video camera that projected the image onto an adjacent colour monitor. An unbiased sampling frame of known area was drawn on a transparency sheet and superimposed on the monitor. Each section was sampled systematically (e.g. every 10th area) with a random start. For each cortical region, the area of the unbiased sampling frame used and the sampling interval through each section is listed in Table 4. For each area sampled, neurons were counted only if the neuron fell inside the sampling frame, did not touch the exclusion lines and came into focus through a certain distance (i.e. the disector height, h) in the middle of each section. The disector height for each cortical region for each staining is listed in Table 4. The number of neurons (Q^-) in a disector volume [$V_{(dis)}$] in the section was obtained. The $V_{(dis)}$ was determined by multiplying the area of the disector frame [a(frame)], which was corrected for magnification, by the disector height (h). Thus, $\Sigma V_{(dis)} = ha$(frame). Then, the total value of neuronal density (N_v) in the region of interest for an individual was determined from the formula: $N_v = \Sigma Q \,/\, \Sigma V_{(dis)}$.

Statistical analysis

The precision of the estimates made on each case could be estimated with data derived from the set of systematically sampled sections of each case (West and Gundersen, 1990). This precision is termed the coefficient of error and was calculated for the total number of points counted over the sectional profiles of the reference volume (ΣP), and the total number of neurons (N). The coefficients of error were calculated using a revised Matheron's quadratic approximation formula described in Gundersen *et al.* (1999). The average coefficient of error for each volume, and for the total number estimate, for each control and Huntington's disease group was calculated using the formula coefficient of error $= (1/n \; \Sigma_i \; CE_i^2)^{1/2}$, where n is the number of cases (West and Gundersen, 1990; Gundersen *et al.*, 1999).

Table 3 Real interpoint distance and the real area of each point used for Cavalieri's estimate of the total volume of each cortical region

Region	Real interpoint distance (mm)	Real area of each point (mm^2)
Primary motor cortex (BA 4)	2.717	7.38
Anterior cingulate cortex (BA 24)	2.000	4.00

BA = Brodmann area.

Table 4 Real sampling frame area, sampling interval and disector height used for the estimate of N_v by the optical disector method for neurons stained with NeuN and SMI32 in various cortical regions

Region	NeuN			SMI32		
	Real sampling frame area (mm^2)	Sampling interval	Disector height (mm)	Real sampling frame area (mm^2)	Sampling interval	Disector height (mm)
Primary motor cortex (BA 4)	0.002	1/10th	0.006	0.0037	1/10th	0.006
Anterior cingulate cortex (BA 24)	0.0017	1/10th	0.008	0.0037	1/10th	0.008

The average data resulting from the neuronal cell estimates for the entire tissue block (within Brodmann area 4 in the primary motor cortex and within Brodmann area 24 in the anterior cingulate cortex) were analysed between groups using analysis of variance (ANOVA). A statistical package for social scientists (SPSS), version 12 was used for these ANOVA analyses. Comparison of specific interest groups was analysed using Bonferroni's *post hoc* test.

The formula for Bonferroni's *post hoc* test =

$$\frac{(\mu_1 - \mu_2)}{\{\mathrm{EMS}[(1/n_1) + (1/n_2)]\}^{1/2}}$$

where μ_1 is the larger and μ_2 is the smaller of the group means, which correspond to the sample size n_1 and n_2, respectively. The EMS is the error mean square which was derived by: EMS = error of the sum of squares/degrees of freedom for this error.

This value of error mean square was obtained from the SPSS version 12 computer output.

Correlation of neuroanatomy and the number of CAG repeats

For each Huntington's disease case, the number of CAG repeats in both alleles of the *HD* gene was determined by polymerase chain reaction amplification of DNA as previously described (Whitefield *et al.*, 1996). The DNA for amplification was isolated either from blood samples or from cerebellar brain tissue from the same Huntington's disease cases.

Methods to assess clinical symptomatology

Clinical data were collected retrospectively from family members of the 12 individuals who had died with Huntington's disease and whose families had requested donation of their brain tissue to the Neurological Foundation of New Zealand Human Brain Bank. The clinical data were collected as part of a larger study using a semi-structured interview and a questionnaire, administered by researchers blind to the neuroanatomical analyses of the brains as previously detailed (van Roon-Mom *et al.*, 2006; Tippett *et al.*, 2007).

The interview format was designed to facilitate the collection of accurate information about the age of clinical onset of Huntington's disease and the patterns of clinical change related to the disease for each Huntington's disease case. Initial questions were open and broad and subsequent questions became more specific, which enabled interviewees to tell their version of events before being exposed to the prompts and possible constraints of specific questions. The Clinical Huntington's disease Questionnaire was developed to provide a comprehensive representation of all reported changes observed in Huntington's disease and an estimate of the severity of impairment in the motor and mood domains of clinical change in the disease, both at clinical onset and near end-stage (see Tippett *et al.*, 2007 for a detailed description). Due to the retrospective aspect of data collection, assessment of cognitive symptoms was not possible. Questions were posed in language that was readily understandable to the lay-person and were administered with the assistance of the researcher who clarified the content of individual items. Any inconsistencies between information given in the semi-structured interview and responses on the questionnaire were investigated at the end of the session.

Total clinical data for each case (i.e. content of the semi-structured interview and responses on the Clinical Huntington's disease Questionnaire) were then viewed independently by two psychologists experienced with Huntington's disease who were blind to the anatomical data obtained for the Huntington's disease cases. They classified each case according to whether motor symptoms were dominant during the course of the disease, mood symptoms were dominant, or both types of symptoms were significant. Definitions used for these classifications were as follows.

Motor: motor symptoms were present with no significant presence of mood symptoms during the disease course.

Mood: mood disturbance was a dominant clinical feature of Huntington's disease across the disease course of the individual. There was, however, almost always some degree of motor symptomatology as well, but these symptoms were either very mild, or, only emerged in the very late stages of the disease.

Mixed motor–mood: significant levels of both symptom-types were present during a large part of the disease.

The classifications of the two psychologists were concordant for 90% of cases in the larger study. For any case where there was a difference, the case materials were reviewed by both psychologists until a consensus was reached.

Results

Overall cell loss in the motor and cingulate cortices in Huntington's disease

In order to investigate the overall cell loss in the primary motor cortex and anterior cingulate cortex in Huntington's disease, the average total number of cells in a tissue block from each cortical region was measured using unbiased stereological counting techniques in 12 cases of Huntington's disease and in 15 controls, matched for sex, age and post-mortem delay. There was a significant overall total neuronal cell loss in both Brodmann area 4 of the primary motor cortex and Brodmann area 24 of the anterior cingulate cortex in Huntington's disease compared to controls (Fig. 2A). In the primary motor cortex (Fig. 2A), there was an average cell loss of 24% ($P < 0.002$, single-factor ANOVA test) in the Huntington's disease cases whereas in the anterior cingulate cortex (Fig. 2A) there was a more pronounced cell loss averaging 36% ($P < 0.0005$). The subpopulation of SMI32-positive pyramidal neurons showed a similar pattern of cell reduction in both the primary motor cortex and the anterior cingulate cortex in Huntington's disease (Fig. 2B) compared to the control cases. On average, there was a significant pyramidal cell reduction of 27% ($P < 0.03$) in the primary motor cortex (Fig. 2B) and a reduction of 34% ($P < 0.003$) in the anterior cingulate cortex in Huntington's disease (Fig. 2B). These results are consistent with the findings from an analysis of the absolute number of neurons in the entire primary motor cortex in Huntington's disease versus control cases (Macdonald and Halliday, 2002). These results are also consistent with the findings from an analysis of the number of SMI32-positive neurons per length of cerebral cortex in the anterior cingulate cortex for Huntington's disease versus control cases (Cudkowicz and Kowall, 1990). Since there is a reduction in grey

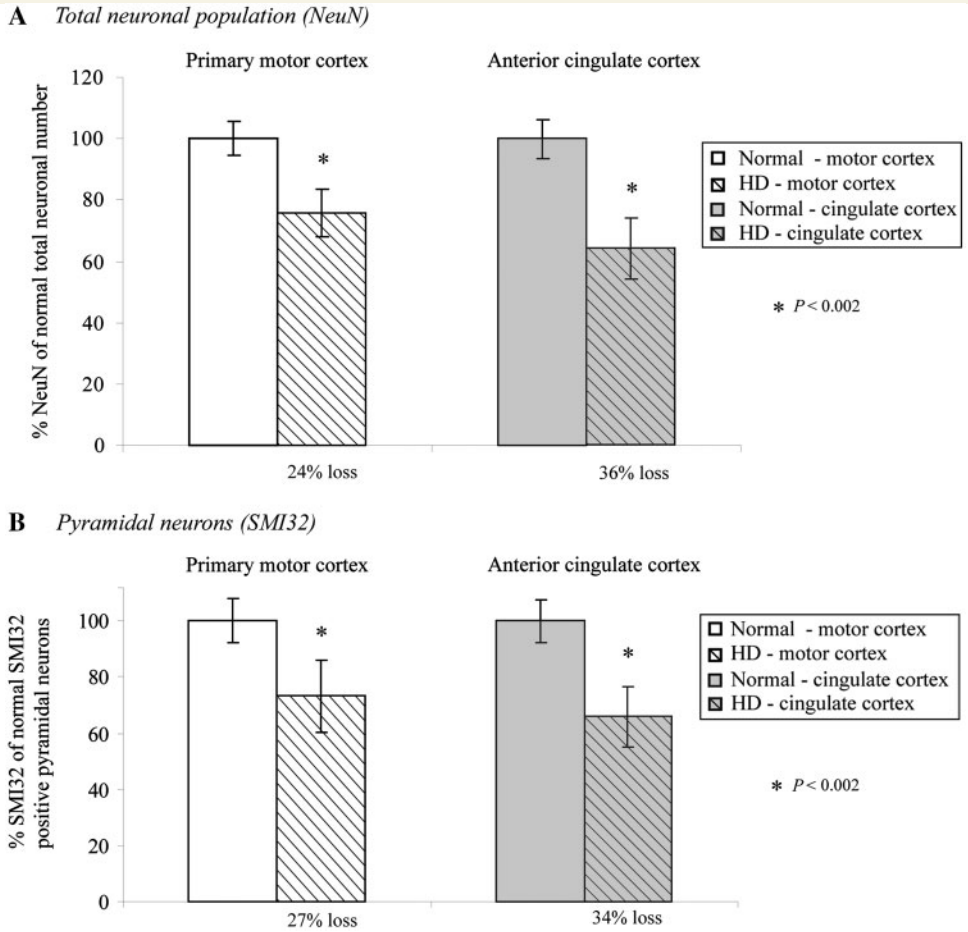

Figure 2 Graphs showing the total average number of (**A**) NeuN-positive neurons and (**B**) SMI32-positive pyramidal neurons in a defined volume of Brodmann area 4 of the primary motor cortex and in a defined volume of Brodmann area 24 of the anterior cingulate cortex in 12 Huntington's disease cases compared to 15 control cases. In the Huntington's disease cases, there is (**A**) an average total cell loss of 24 ± 8% (mean ± SEM) in the primary motor cortex and 36 ± 10% in the anterior cingulate cortex, and (**B**) an average pyramidal cell loss of 27 ± 13% in the primary motor cortex and an average cell loss of 34 ± 11% in the anterior cingulate cortex. Asterisks indicate statistically significant difference from the control ($P < 0.002$) using single factor ANOVA test.

matter volume of the frontal cortex in Huntington's disease rather than an increased volume due to gliosis (e.g. Halliday *et al.*, 1998), a reduced number of neurons in a subvolume, or per length of cerebral cortex, compared to control cases is likely to be a real biological decrease.

For all stereological analyses for the control and Huntington's disease cases, the average coefficient of error for the reference volume [i.e. CE(ΣP)] was less than 0.08 and the average coefficient of error for the total number of neurons [i.e. CE(N)] was mostly less than 0.10 and always less than 0.13. This indicates that the estimates of reference volume and total neuronal number were generally reliable (i.e. CE $\leqslant$ 0.10). For all analyses, the observed mean variance of the individual total number estimates (i.e. CE^2) was less than half of the observed mean variance of the group (i.e. the coefficient of variation, CV^2). This indicates that the variability is due to a true difference between cases in the total neuronal number rather than a lack of precision in the stereological counting methods employed (West and Gundersen, 1990).

Variation in the cortical cell loss between Huntington's disease cases

There was considerable variation between the 12 individual Huntington's disease cases in the percentage of total neuronal and pyramidal cells lost in both the primary motor cortex and anterior cingulate cortex. As detailed in Fig. 3A, in the motor cortex the total neuronal loss varied from around 50% in four cases (HC60, HC72, HC73, HC93) to 6–28% loss in seven cases (HC68 HC79, HC85, HC95, HC99, HC101, HC107), with one case (HC82) showing no significant cell loss. Similarly, in the cingulate cortex, where the cell loss was generally more extensive, the percentage cell loss varied from around 65% in two cases (HC95, HC101), 42–49% in five cases (HC79, HC82, HC85, HC93, HC107), 18–31% in 3 cases (HC60, HC72, HC99), with no significant cell loss in two cases (HC68, HC73; Fig. 3A). Similar trends were also observed in the pattern of pyramidal cell (SMI32) loss; comparison between Huntington's disease cases showed that the pyramidal cell loss varied in the motor cortex from 59% to no

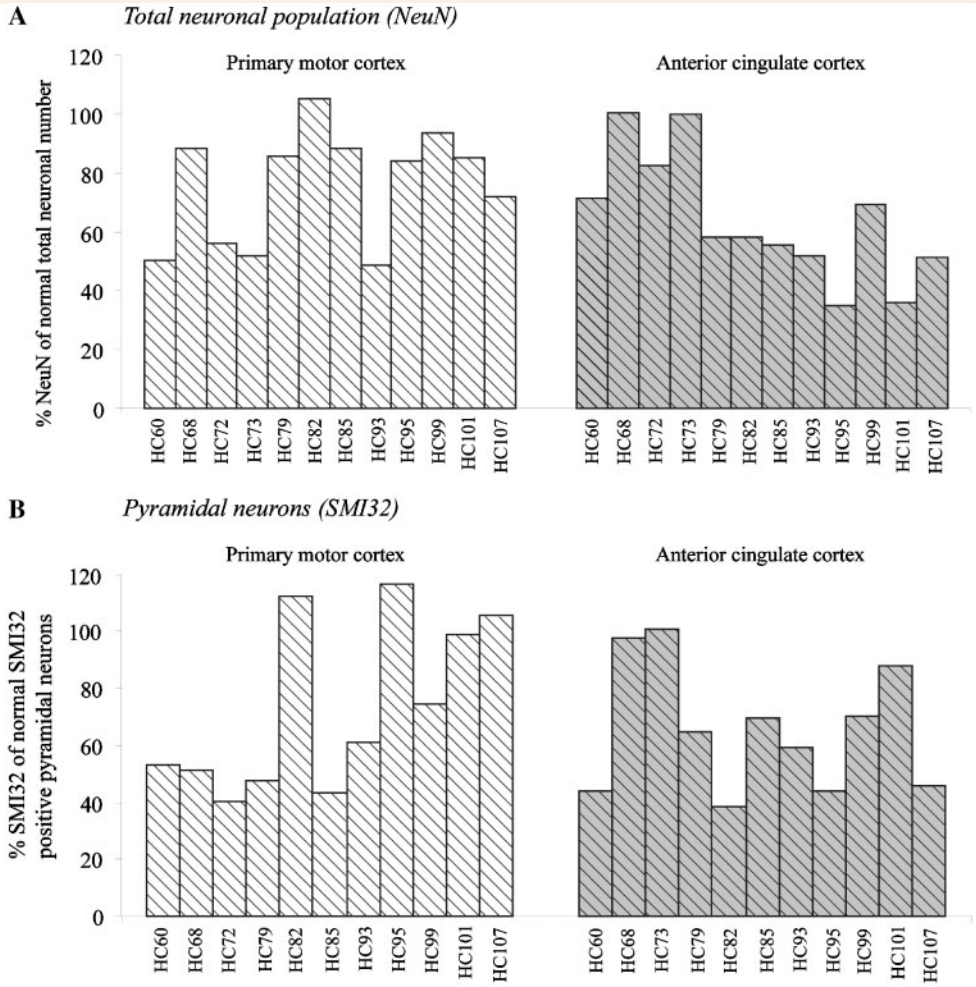

Figure 3 Graph showing the variation of (**A**) total number of NeuN-positive neurons and (**B**) SMI32-positive pyramidal neurons expressed as a percentage of control in Brodmann area 4 of the primary motor cortex and Brodmann area 24 of the anterior cingulate cortex between the Huntington's disease cases.

cell loss, and in the cingulate cortex from 61% to no cell loss (Fig. 3B).

Most interestingly, the total cell loss and pyramidal cell loss in the motor cortex did not always follow the pattern of cell loss in the cingulate cortex (Fig. 3A and B). That is, some cases which showed major cell loss in the motor cortex showed minimal cell loss in the cingulate cortex (e.g. HC73); other cases showed the reverse trend (e.g. HC82) and some showed similar patterns of loss in both cortical regions (e.g. HC93).

Relation between clinical symptoms and differential cell loss in the cerebral cortex

We next investigated whether the variation in the pattern of cell loss in the motor cortex and cingulate cortex was related to the variation in symptomatology. We found marked heterogeneity in the symptoms expressed by the Huntington's disease patients during the course of the disease. Using the criteria described in the methods, of the 12 Huntington's disease cases in this study (Table 1), four cases were classified as motor cases (HC68, HC72, HC73, HC99), four were classified as mood cases (HC82, HC85, HC95, HC101) and four were classified as mixed cases, with significant levels of both symptom-types present during a large part of the disease course (HC60, HC79, HC93, HC107). To test whether the differential cortical cell loss between the motor and cingulate cortices was related to the different symptom subtypes exhibited by the different cases, the blinding of the clinical and anatomical assessments was broken, and we compared the average total cell loss and pyramidal cell loss of the cases in each of the three phenotypic groups (motor, mood and mixed motor–mood symptom groups, Fig. 4).

Comparison of the total cell loss in the primary motor cortex and anterior cingulate cortex, in the groups comprising motor or mood cases, showed a clear association between cell loss and symptom phenotype (Fig. 4). In the group of Huntington's disease cases who experienced mainly motor symptoms, major cortical cell loss was found in the motor cortex [average cell loss of 28% ($P < 0.02$, Bonferroni's *post hoc* test)] with no significant cell loss

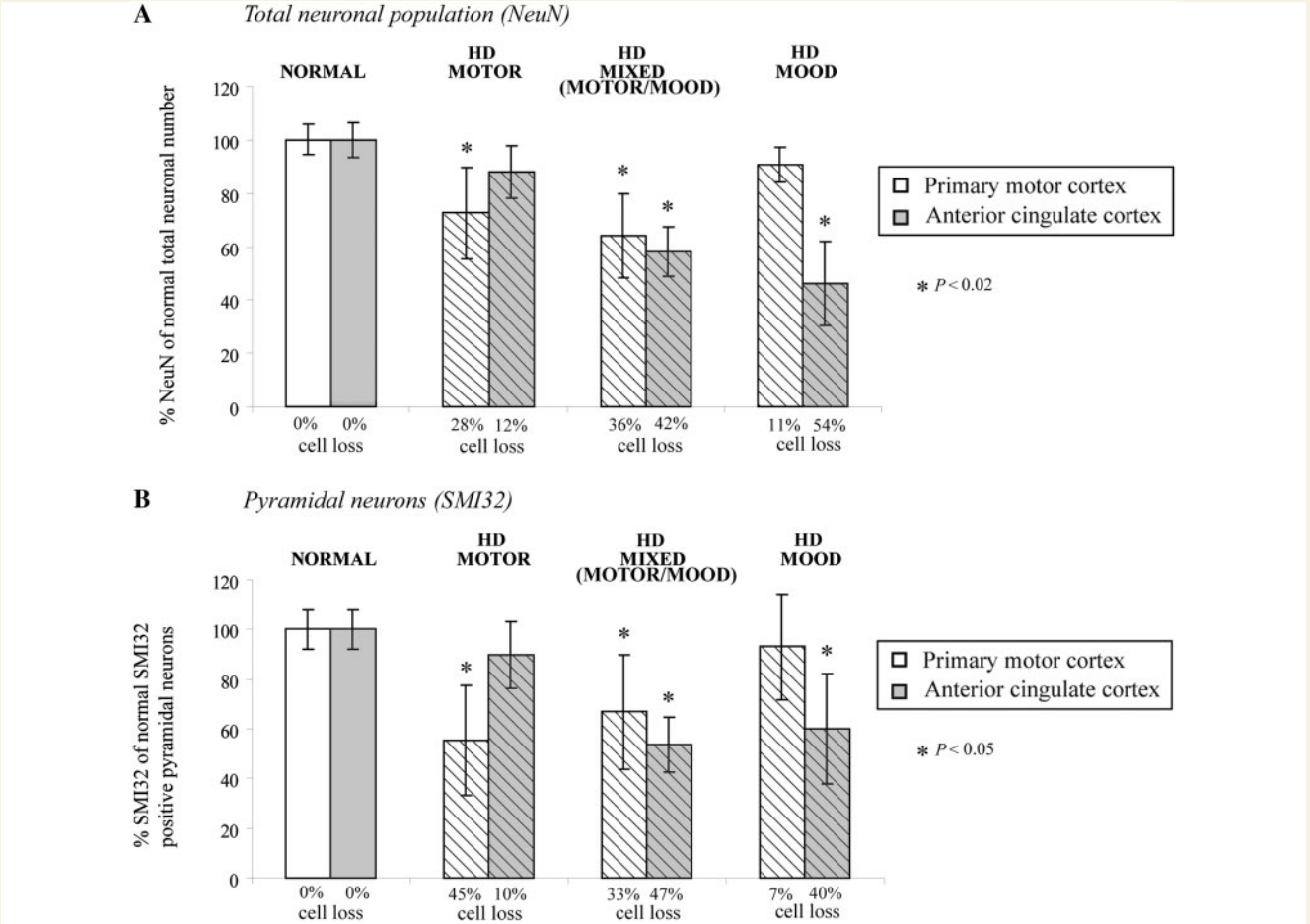

Figure 4 Graph showing (**A**) the total number of NeuN-positive neurons and (**B**) SMI32-positive pyramidal neurons (expressed as a percentage of the control) in the primary motor cortex and the anterior cingulate cortex of the three different symptom profile groups of Huntington's disease cases (HD; motor, mixed and mood). Asterisks indicate statistically significant differences from the control ($P < 0.05$) using the Bonferroni *post hoc* test. Note that the cell loss in the primary motor cortex shows an opposite trend to the anterior cingulate cortex across the three Huntington's disease symptom groups.

in the cingulate cortex (Fig. 4A). In contrast, in the Huntington's disease group where mood was the major phenotype of the cases, an extensive cell loss averaging 54% ($P < 0.0002$) was found in the cingulate cortex with no significant cell loss in the motor cortex (Fig. 4A). In agreement with this general pattern, the group showing a mixed motor–mood symptomatology showed an extensive cell loss in both the motor cortex (36%, $P < 0.002$) and the cingulate cortex [42% ($P < 0.001$), Fig. 4A].

Furthermore, the pattern of cell loss of SMI32-positive pyramidal cells in the motor and cingulate cortices in the mainly motor and mood phenotypic groups (Fig. 4B) closely follows the pattern seen in the total neuronal loss (Fig. 4A); there was a significant major loss of pyramidal cells in the motor symptom group in the motor cortex (45%, $P < 0.05$) with no significant loss in the cingulate cortex (Fig. 4B). The reverse profile applied in the mood subgroup which showed a major pyramidal cell loss in the cingulate cortex (40%, $P < 0.05$) with no significant cell loss in the primary motor cortex (Fig. 4B). Similar to the pattern of total neuronal cell loss, the group of cases showing a mixed motor–mood phenotype collectively showed a significant pyramidal cell loss in both the primary motor cortex (33%, $P < 0.05$) and anterior cingulate cortex [47%, ($P < 0.05$), Fig. 4B].

Examination of the cell morphology at high magnification at five representative levels of each cortical block showed the presence of major morphological cell changes in the remaining neurons of the affected cortical regions (Figs 4–6). In all of the cases in the motor and mixed motor–mood phenotype groups, which both showed marked total and pyramidal cell losses in the primary motor cortex, many of the surviving cortical neurons showed marked dystrophic changes suggestive of ongoing pathology (Fig. 5). This was most clearly seen in the surviving pyramidal neurons in layers III and V stained with NeuN and SMI32 which showed marked shrinkage of the cell bodies and extensive loss of dendritic staining (both apical and basal dendrites) (Fig. 5B, C, F and G). In contrast, no obvious change in the neuronal morphology was apparent in the surviving neurons (Fig. 5D and H) in cases with dominant mood symptomatology in which there was no significant cell loss in the motor cortex (Fig. 4). Similar clear-cut morphological changes were also seen in the anterior cingulate cortex of cases with mood symptoms. In all of the mood and mixed mood/motor cases where the

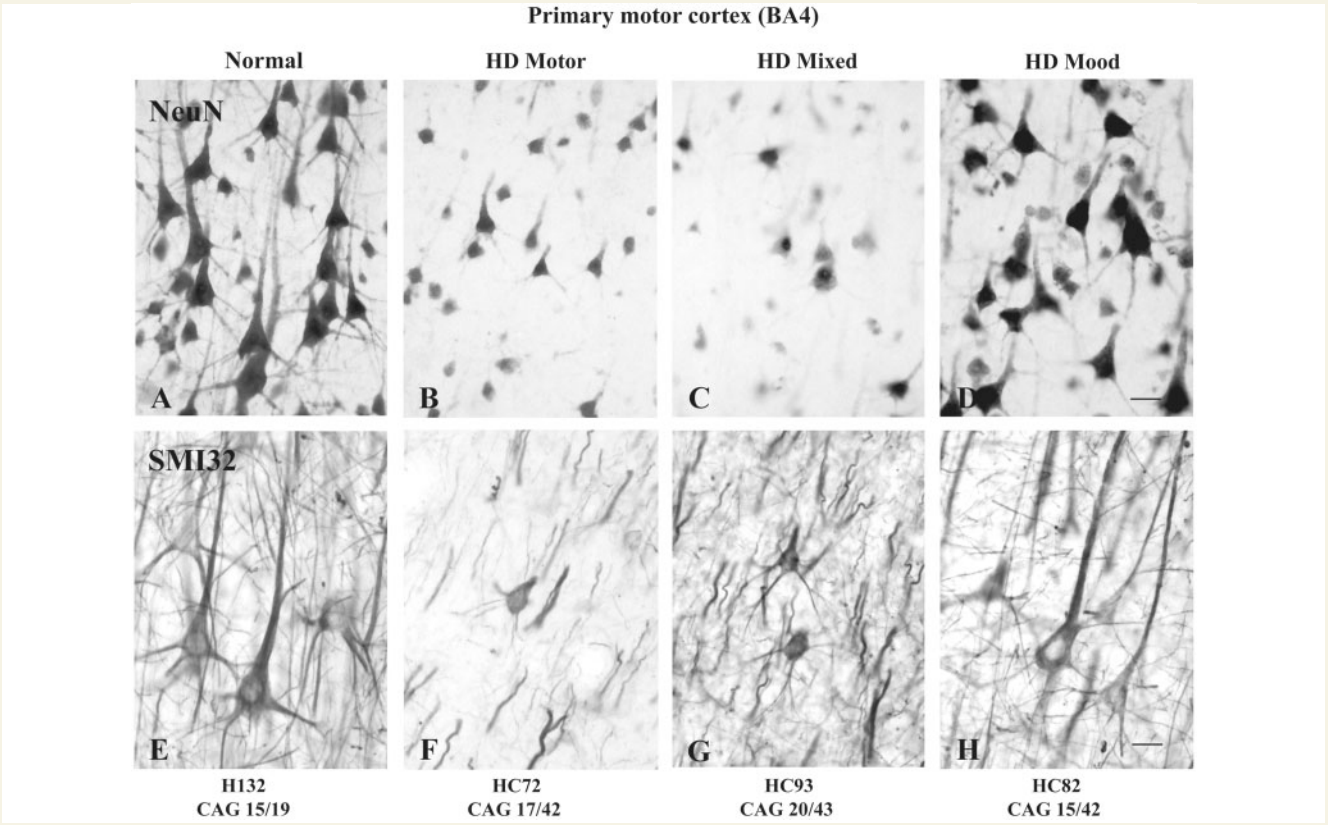

Figure 5 Photomicrographs illustrating the pyramidal neurons in layer III in Brodmann area 4 of the primary motor cortex of control (**A**, **E**) and Huntington's disease (**B–D**, **F–H**) cases (HD) with mainly motor (**B**, **F**), mixed (motor–mood) (**C**, **G**) and mainly mood (**D**, **H**) symptom profiles. Note that the Huntington's disease cases all have a similar number (42 and 43) of CAG repeats on the *HD* allele of the IT15 gene. **A–D**, Pyramidal neurons in layer III of Brodmann area 4 stained with NeuN. **E–H**, Pyramidal neurons in layer III of Brodmann area 4 stained with SMI32. Scale bars, **A–D** and **E–H** = 30 μm.

cingulate cortex showed major and selective cell loss (Fig. 4), many of the surviving neurons also showed dystrophic changes (Fig. 6C, D, G and H) similar to those seen in the motor cortex of the motor phenotype cases. In contrast, in the cases of mainly motor symptomatology where there was no significant cell loss in the cingulate cortex, no or minimal change in the morphology of the neurons was shown in the remaining neurons (Fig. 6B and F).

Relation between the pattern of cell loss in the cerebral cortex and striatal neuropathological grades

In this study, the 12 Huntington's disease cases exhibited a range of striatal neuropathological grades as determined by the Vonsattel criteria (Table 1). In order to investigate if there was any relationship between the pathology of the cerebral cortex and the overall pathology of the striatum, we investigated whether there was any relation between the extent of cortical cell loss and the striatal Vonsattel neuropathological grades (Fig. 7).

Analyses of total neuronal cell loss in the motor and cingulate cortices (compared to the control brains) revealed a variable neuronal cell loss in both cortical regions in the different striatal neuropathological grades of the Huntington's disease cases (Fig. 7A). In general terms, the pattern of average cell loss in the primary motor cortex appeared to parallel the overall increasing striatal neuropathological grades (Fig. 7A). There was no significant cell loss in the motor cortex in the Grades 0–1 group, but there was significant neuronal loss in the motor cortex in the higher neuropathological grades, which showed an increasing trend from Grade 2 (22%, $P<0.02$) to Grade 3 (35%, $P<0.002$). By contrast, neuronal loss in the anterior cingulate cortex showed a different pattern with a less apparent correlation to neuropathological grade (Fig. 7A). There was a dramatic and significant cell loss in the cingulate cortex across all Huntington's disease grades compared to the control with average cell losses of 35% ($P<0.05$) in Grades 0–1, 31% in Grade 2 ($P<0.02$) and 42% in Grade 3 ($P<0.002$) (Fig. 7A).

As shown in Fig. 7B, there was a variable cell loss of SMI32-positive pyramidal neurons in the primary motor cortex and the anterior cingulate cortex in Huntington's disease across the various striatal neuropathological grades. For the motor cortex, there was a significant cell loss only at Grade 3, 34% ($P<0.05$) (Fig. 7B). In contrast, the cingulate cortex showed a pattern of pyramidal cell loss which corresponded with the striatal

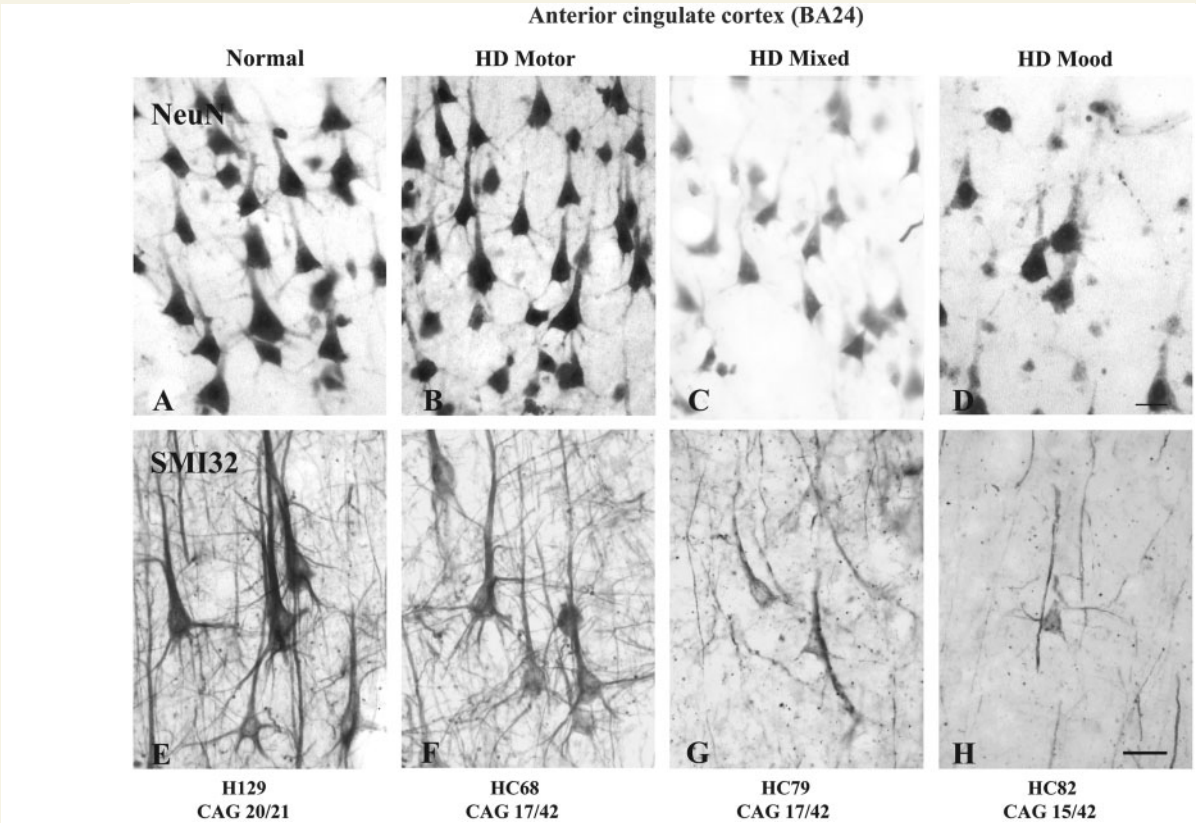

Figure 6 Photomicrographs illustrating the pyramidal neurons in layer III in Brodmann area 24 of the anterior cingulate cortex of control (**A** and **E**) and Huntington's disease (**B–D**, **F–H**) cases (HD) with 'mainly motor' (**B** and **F**), 'mixed' (motor–mood) (**C** and **G**) and 'mainly mood' (**D** and **H**) symptoms. Note that the Huntington's disease cases all have the same number (42) of CAG repeats on the Huntington's disease allele of the IT15 gene. (**A–D**) Pyramidal neurons in layer III of Brodmann area 24 stained with NeuN. (**E–H**) Pyramidal neurons in layer III of Brodmann area 24 stained with SMI32. Scale bars, **A–D** and **E–H** = 30 μm.

neuropathological grades, with significant losses evident at the higher neuropathological grades, 36% ($P < 0.05$) in Grade 2 and 45% ($P < 0.002$) in Grade 3 (Fig. 7B).

Comparison of the cell loss in the cerebral cortex with the number of CAG repeats in the *HD* gene

We next investigated whether the total cell loss and pyramidal cell loss in the primary motor and anterior cingulate cortices correlated with the CAG repeat lengths in the *HD* gene. As shown in Fig. 8A and B, there were no significant correlations between the CAG repeat number and total cell loss in either primary motor cortex ($r^2 = 0.1948$, $P = 0.1509$) or anterior cingulate cortex ($r^2 = 0.1858$, $P = 0.1618$, Fig. 8B), although there appeared to be a trend towards increasing cell loss with increasing CAG repeats in both cortical areas. The correlations between the number of CAG repeats and the loss of SMI32-positive pyramidal cells were also not significant in either the primary motor cortex ($r^2 = 0.1101$, $P = 0.3188$, Fig. 9A) or the anterior cingulate cortex ($r^2 = 0.3215$, $P = 0.0689$, Fig. 9B).

Discussion

Our results suggest that in Huntington's disease, cell loss in two functionally diverse regions of the cerebral cortex—the primary motor cortex and anterior cingulate cortex—is associated with motor and mood symptomatology, respectively. This detailed stereological study of 12 post-mortem Huntington's disease brains revealed a major cell loss in these two cortical regions, but interestingly, showed that there is marked variation in the extent of cell loss between individual Huntington's disease cases. The most striking finding of the study is that the heterogeneous pattern of cell loss in the motor and cingulate cortices in different Huntington's disease cases corresponds to the variable pattern of motor and mood symptoms presented clinically in these cases. The general implication of our results is that the expanded CAG sequence in the *HD* gene can produce variable topographical patterns of cortical neuronal degeneration that contribute to specific symptoms. The relationship demonstrated between symptom profiles and cortical degeneration provides a novel perspective on understanding the neural basis of clinical heterogeneity found in Huntington's disease.

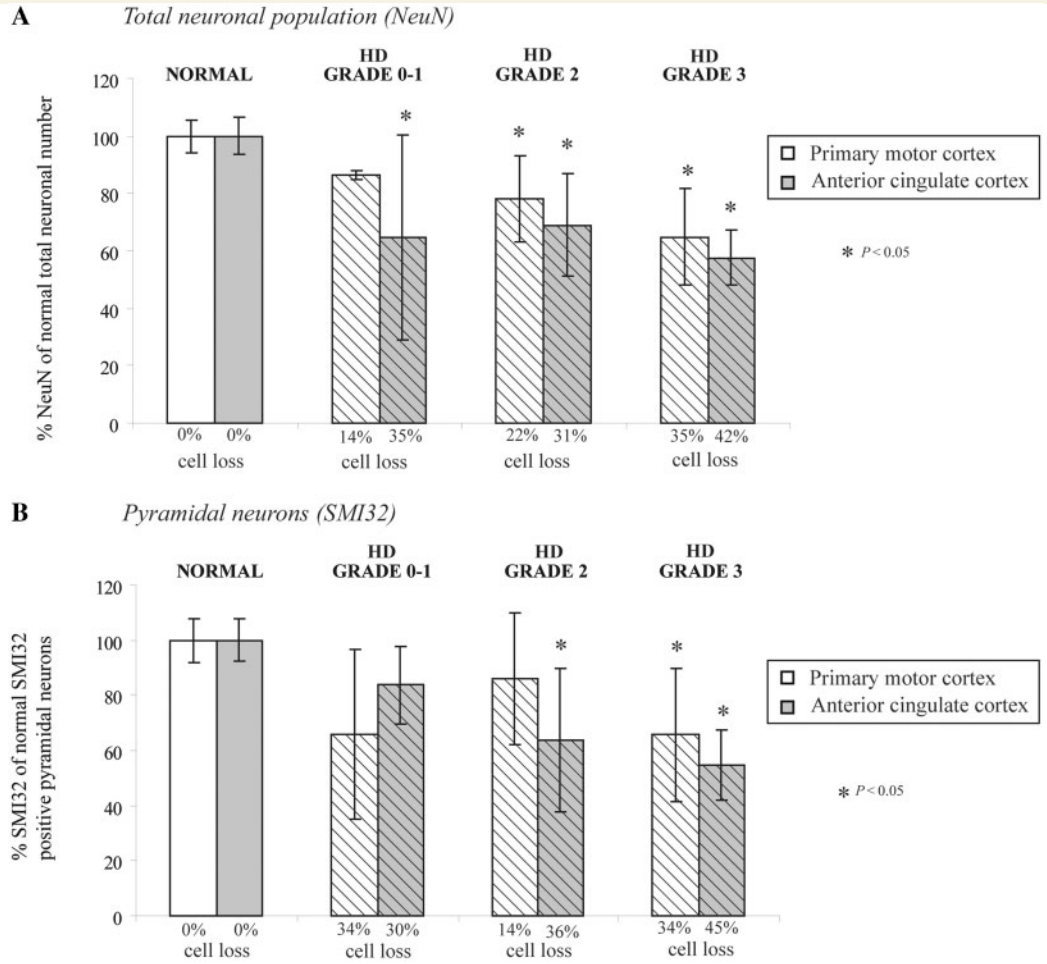

Figure 7 Graphs showing the total average number of (**A**) NeuN-positive neurons and (**B**) SMI32-positive pyramidal neurons (expressed as a percentage of the control) in the primary motor cortex and the anterior cingulate cortex with increasing striatal neuropathological grades (Grades 0–3). Asterisks indicate statistically significant differences from the control ($P < 0.05$) using the Bonferroni *post hoc* test. HD = Huntington's disease cases.

Cell loss in the cerebral cortex in Huntington's disease

Our studies demonstrating marked neuronal loss throughout the motor and cingulate cortices in Huntington's disease complement and extend the considerable literature showing cortical degeneration throughout many regions of the cortex, such as decreases in post-mortem cortical volume (Mann *et al.*, 1993; Halliday *et al.*, 1998) and neuronal loss and morphological changes (de la Monte *et al.*, 1988; Hedreen *et al.*, 1991; Sotrel *et al.*, 1991, 1993; Heinsen *et al.*, 1994; Macdonald *et al.*, 1997; Macdonald and Halliday, 2002; Rosas *et al.*, 2002, 2008; DiProspero *et al.*, 2004; Selemon *et al.*, 2004). However, of these previous studies only two quantitatively examined cell loss in the motor or cingulate cortices (Cudkowicz and Kowall, 1990; Macdonald and Halliday, 2002).

Our study showed that there is an overall significant loss of 24% of the total neuronal population and 27% loss of SMI32-positive pyramidal cells in the Huntington's disease primary motor cortex is in general agreement with the previous quantitative study, which showed a major depletion of the total neuronal number (42%) and SMI32-positive pyramidal neurons (41%) in the primary motor cortex of five Grades 2–3 Huntington's disease cases (Macdonald and Halliday, 2002). Secondly, our studies in the anterior cingulate cortex showed an average 36% total neuronal loss and a 34% loss of SMI32-positive pyramidal cells in Grades 1–3 Huntington's disease cases; Cudkowicz and Kowall (1990) previously found a significant loss of 25% of SMI32-positive pyramidal neurons in the cingulate cortex in Grade 2–4 Huntington's disease cases, although Macdonald and Halliday (2002) found no significant change in the total neuronal number in the *motor* cingulate cortex (i.e. the posterior part of Brodmann area 24) in Grades 2–3 Huntington's disease cases (Macdonald and Halliday, 2002).

While our findings of an extensive and significant cell loss in the motor and cingulate cortices in Huntington's disease are in general agreement with the results of prior studies of cortical degeneration in Huntington's disease, our study demonstrates that there is a surprisingly high variation in the extent of cell loss between the cases that has not been highlighted in previous reports. Comparison between Huntington's disease cases in our study shows a marked variation in the degree of both the total cell

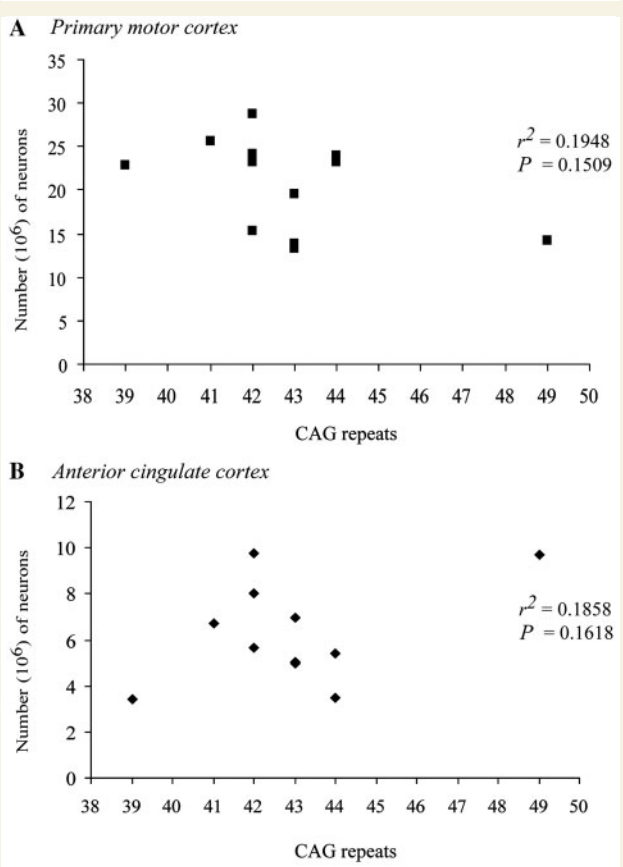

Figure 8 Comparison of total neuronal number (NeuN) in the (**A**) primary motor cortex and (**B**) anterior cingulate cortex with the number of CAG repeats in the IT15 gene in the Huntington's disease cases. There is no significant correlation between the CAG repeats and the total number of neurons.

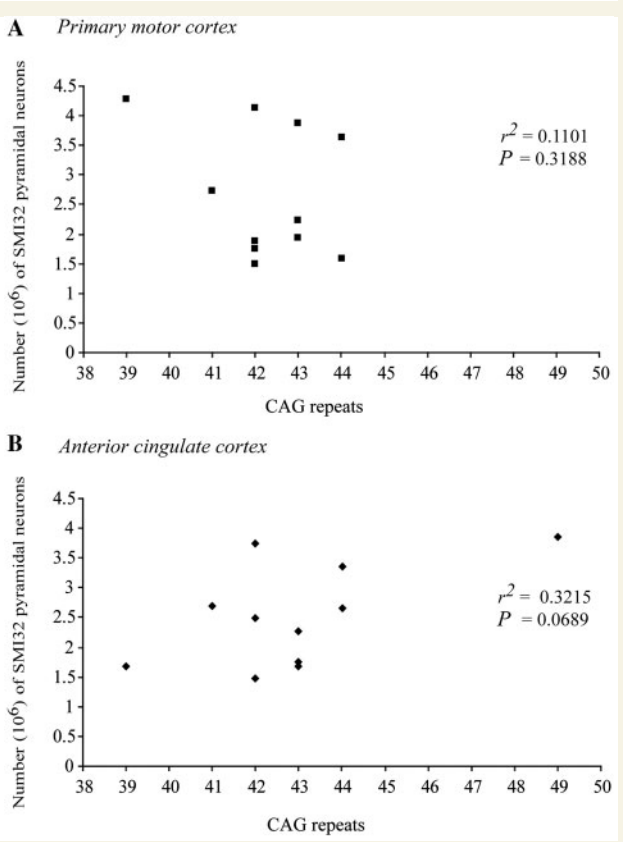

Figure 9 Comparison of the number of SMI32-positive pyramidal neurons in the (**A**) primary motor cortex and (**B**) anterior cingulate cortex with the number of CAG repeats in the IT15 gene in the Huntington's disease cases. There is no significant correlation between the CAG repeats and the number of SMI32-positive pyramidal neurons.

and pyramidal cell loss in the primary motor cortex (0–51% loss) and the anterior cingulate cortex (0–65% loss). Most interestingly, we found no association between the pattern of cell loss in the motor cortex and cingulate cortices across the Huntington's disease cases. In addition, the cell loss in the total neuronal population and in the SMI32-positive pyramidal neurons varied from case to case within each cortical region, although in most cases the pattern of pyramidal cell loss did follow the trend of total cell loss (Fig. 2) confirming previous studies showing that pyramidal cells are the major cell type in the cerebral cortex which are affected in Huntington's disease (Cudkowicz and Kowall, 1990; Hedreen *et al.*, 1991; Macdonald *et al.*, 1997; Macdonald and Halliday, 2002). This between-case variation in the pattern of cell loss is a novel and characteristic feature of our results showing that there is considerable heterogeneity in the pattern of cortical neuronal degeneration in Huntington's disease. Since it is well established that there is also variation in symptom profile in Huntington's disease, then, as discussed below, the next step was to investigate whether this marked variation in cell loss in the motor and cingulate cortices in Huntington's disease cases may be related to the variation in symptomatology.

Relationship of cortical cell loss to clinical symptom profile

Huntington's disease is characterized by a diverse range of symptoms including motor, mood and cognitive disturbances, which vary between patients (Gusella, 1991; Zappacosta *et al.*, 1996; Vonsattel and DiFiglia, 1998). Recently, several different imaging studies in patients with Huntington's disease have suggested that cortical changes may play a crucial role in the development of clinical symptoms (see Paulsen, 2009 for a review). Studies using functional MRI have identified cortical regions of lower and higher activation in early and premanifest Huntington's disease during performance on a variety of cognitive tasks (Kim *et al.*, 2004; Wolf *et al.*, 2008), with two studies also demonstrating an association between poor task performance and changes in functional connectivity between cortical regions (Thiruvady *et al.*, 2007; Wolf *et al.*, 2008). These findings concur with results from studies using structural MRI, most significantly those of Rosas *et al.* (2005, 2008), who measured cortical thinning in pre- and early Huntington's disease patients using high-resolution surface based analysis of *in vivo* MRI data. The authors found greater cortical thinning in Huntington's disease patients with reduced functional

scores, and heterogeneous regional patterns of cortical thinning between cases which correlated with heterogeneity in clinical profile (Rosas *et al.*, 2002, 2005, 2008). As highlighted by Paulsen (2009), however, imaging data to date still do not resolve the issue as to whether or not changes in cortical activation or thickness directly reflect death or dysfunction in cells in those regions, or whether they reflect dysfunction from striatal alterations (Paulsen, 2009). Our findings add strong support for the role of cortical pathology in the expression of clinical symptoms in Huntington's disease by demonstrating a clear association between the pattern of cortical neuronal loss in post-mortem Huntington's disease brains and the pattern of clinical symptomatology experienced by those individuals during the course of the disease.

In our study, we showed that in the primary motor cortex there was a significant loss of total neurons and SMI32-positive pyramidal neurons in Huntington's disease cases with a dominant motor symptom phenotype (but not in cases with a dominant mood phenotype), which parallels the established role of the primary motor cortex in voluntary movements. In contrast, the anterior cingulate cortex exhibited a significant total cell and pyramidal cell loss in the Huntington's disease cases with a dominant mood phenotype but not in cases with dominant motor phenotype. The anterior cingulate cortex is one of the major components of the limbic system and may play an important role in both mood and cognitive impairment (Davidson *et al.*, 2002; Georgiou-Karistianis *et al.*, 2007; Thiruvady *et al.*, 2007; Alexopoulos *et al.*, 2008). Our previous study on the basal ganglia has shown a greater mood dysfunction associated with greater damage to the striosome compartment of the striatum (Tippett *et al.,* 2007), which receives input from the limbic related cortical areas including the anterior cingulate cortex (Eblen and Graybiel, 1995). This suggests that the profile of mood symptoms in Huntington's disease is likely to be associated with degeneration in limbic regions with extensive projections to the striatum. Thus, our results showing a variable pattern of neurodegeneration in the two cortical regions studied provide evidence suggesting a significant association between neuronal degeneration in the human cerebral cortex and the symptom profile in Huntington's disease.

The correlation of the clinical symptom profiles in Huntington's disease with the cortical pathology was not only shown by the pattern of cell loss but also in the dystrophic morphology of the surviving neurons in the two cortical regions. In both the motor and cingulate cortices, pyramidal neurons were particularly affected, with major morphological changes evident, including cell shrinkage and loss of stained dendritic processes in the corresponding symptom profile cases—i.e. the most marked dystrophic changes in the motor and cingulate cortices were seen in those cases with the most marked motor and mood symptom profiles. Morphological changes in the pyramidal cells including dendritic remodelling, altered size and number of dendritic spines have been previously observed in Huntington's disease cortex prior to degeneration (Sapp *et al.*, 1997) and transgenic mouse models of Huntington's disease (Laforet *et al.*, 2001). The observation of marked neuronal dystrophic changes correlating with symptom profile in our studies provides suggestive evidence for ongoing progressive neuronal dysfunction and physiological stress in the cerebral cortex which may contribute to the variable developing symptom phenotypes seen in Huntington's disease.

Relationship of cortical cell loss to striatal degeneration and neuropathological grade

The extensive anatomical connections between the cerebral cortex and the striatum through the topographically organized corticostriate projection make it very difficult to define how dysfunction and degeneration in the cerebral cortex and the striatum, alone or in combination, contribute to symptom profile. Nevertheless, comparison of cortical cell loss in Huntington's disease cases with striatal neuropathological grade may well shed light on the pathogenesis. In our study, the neuronal cell loss in the primary motor cortex generally increased with increasing striatal neuropathological grades suggesting a close relationship between cortical and striatal degeneration; this is consistent with Macdonald and Halliday (2002) who found major cortical neuronal loss of greater than 40% in Grades 2–3 Huntington's disease cases. These general findings suggest a linkage of cortical and striatal degeneration. Nevertheless, the finding in our study of significant major cell loss in the cingulate cortex across all striatal neuropathological grades suggests that the degeneration in the cerebral cortex does indeed play a key role in Huntington's disease pathogenesis.

Generally, in our study the pyramidal cell loss in Huntington's disease cases correlated closely with the total cell loss, suggesting that in Huntington's disease mainly projection neurons in layers III, V and VI are affected. This agrees with previous cortical studies (Cudkowicz and Kowall, 1990; Hedreen *et al.*, 1991; Sotrel *et al.*, 1993; Macdonald *et al.*, 1997; Macdonald and Halliday, 2002) showing that the pyramidal cells, which are the major output neurons of the cortex, are the major cortical cell type affected in Huntington's disease. Death of cortical pyramidal cells in the Huntington's disease brain may contribute to dysfunction in other cortical and subcortical regions, particularly the striatum. The dysfunctional changes in corticostriatal projections that occur in Huntington's disease may originate at the level of gene expression. This is supported by our recent microarray analysis of primary motor cortex from 34 Grades 0–2 Huntington's disease cases (including cases used in the present study), which indicated that 3% of mRNAs (1482) were differentially expressed (Hodges *et al.*, 2006). In addition, this study showed greater abnormalities in mRNA expression in the motor cortex than in prefrontal association cortex, demonstrating a regionally distinct pattern of differential expression that may correspond to the severity of effects (or, alternatively, to a heterogeneity of mechanisms) in different cortical regions in Huntington's disease. As a prominent example, it is well established that brain-derived neurotrophic factor, a neurotrophin important for striatal neuron survival (Cattaneo *et al.*, 2001; Ferrer *et al.*, 2001; Zuccato *et al.*, 2001), is produced by cortico-striatal pyramidal projection neurons and transported in an anterograde manner to the striatum (Altar *et al.*, 1997) and that in Huntington's disease, decreases in cortical brain-derived neurotrophic factor gene transcription (Zuccato *et al.*, 2001) and defects in brain-derived neurotrophic factor transport (Gauthier *et al.*,

2004) may result in reduced brain-derived neurotrophic factor trophic support to the striatum leading to striatal neurodegeneration. A recent study of mRNA changes in layer-five projection neurons in the primary motor cortex in Huntington's disease has also shown a decrease in both mRNA and protein levels of Lin7b, a protein involved in neuronal polarity and synaptic connectivity (Zucker *et al.*, unpublished).

Relationship of cortical cell loss to CAG repeat length

We found no significant correlation between CAG repeat numbers and neuronal cell loss in the cortex. This contrasts with findings of a significant relation between CAG repeat numbers and the extent of neuronal loss in the caudate nucleus and the putamen or gross striatal neuropathological grade (Penney *et al.*, 1997; Vonsattel and DiFiglia, 1998). Although this may be due to the small sample size in the present study, it could also suggest that the neurodegeneration in the cortex (unlike the striatum) is not strongly dependent on CAG repeat length. This is supported by our finding that cases with the same number of CAG repeat length showed a marked variation in the extent of cortical cell loss and symptom profiles. In addition, clinical expression of Huntington's disease in monozygotic twins can also be markedly different despite the same number of CAG repeats (Georgiou *et al.*, 1999; Gomez-Esteban *et al.*, 2007), suggesting that the effects of the mutant *HD* gene may be modified by other genetic and environmental factors. Indeed, studies on transgenic animal models of Huntington's disease show that environmental enrichment has a clear influence on neurochemical degenerative changes in the basal ganglia and on symptom progression (van Dellen *et al.*, 2000; Glass *et al.*, 2004; Spires *et al.*, 2004). Also, consideration of the correlation of age of onset with CAG repeat size in Huntington's disease, suggests that 40% of the variability may be accounted for by modifying genes and environmental effects (Wexler *et al.*, 2004). Taken together with our present findings that regional cortical pathologies correlate with specific symptomatologies, it is interesting to consider whether gene and environmental modifier effects may also act on regionally variant substrates to play a role in determining Huntington's disease phenotype characteristics.

Mechanisms of cortical degeneration

The exact mechanisms of neuronal cell death in Huntington's disease are currently unclear but may involve transcriptional dysregulation, excitotoxicity, oxidative stress, changes in neurotransmitters, cortical brain-derived neurotrophic factor production, and breakdown of cellular and vesicular transport mechanisms. Recent transgenic animal studies have implicated dysfunction of the cortex as one of the major indicators of phenotype; this may occur through cortical synaptic dysfunction before cell death (Cepeda *et al.*, 2007; Cummings *et al.*, 2009). Dysfunction of the corticostriatal pathway involves complex and multiple changes that have been documented and which may lead to neurodegeneration of both cortical and striatal neurons; mutant Huntingtin's effects in cortical neurons cause dysfunction of the corticostriatal pathway and dysregulation of neurotransmitter and brain-derived neurotrophic factor release which probably impairs the functioning of the striatal neurons (Cepeda *et al.*, 2007; Strand *et al.*, 2007). Also, abnormal cortical glutamate receptor functions have been implicated in behavioural and motor impairments in transgenic mice with physiological and morphological cortical changes predicting the onset and severity of behavioural deficits (Laforet *et al.*, 2001; Andre *et al.*, 2006). Furthermore, studies in the conditional mouse model where cortical and/or striatal cells selectively expressed mutant Huntingtin, dysfunction of the cortical neurons was essential to the development of significant behavioural and motor deficits (Gu *et al.*, 2007). Other transgenic mouse studies have implicated dysfunction of both the cortical projection and interneurons in the development of Huntington's disease pathology (Gu *et al.*, 2005; Spampanato *et al.*, 2008). All of these animal studies provide accumulating mechanistic evidence that the cortex plays a major role in the initiation and development of the Huntington's disease phenotype, and that dysfunction in the corticostriate neurons plays a central role in Huntington's disease forebrain pathology.

Our studies here in the post-mortem Huntington's disease human brain together with the *in vivo* findings of Rosas *et al.* (2008) in patients with Huntington's disease demonstrate that the heterogeneous pattern of cortical degeneration correlates with phenotype variability and further confirms the determining role of the cerebral cortex in Huntington's disease aetiology and manifestation.

Conclusion

The results of the present study have shown major cell loss in the primary motor and anterior cingulate cortices in Huntington's disease. Loss in the primary motor cortex increases with Huntington's disease grade whereas loss in the anterior cingulate cortex was similar across all grades. Most strikingly, when cases were classified into symptom categories, there was a marked cell loss in the primary motor cortex in cases with prominent motor symptoms and a marked cell loss in the anterior cingulate cortex in cases with prominent mood symptoms. These results provide evidence that the heterogeneity and specific nature of clinical symptomatologies experienced by patients with Huntington's disease can be at least partly accounted for by heterogeneous neurodegeneration in particular functional regions of the cerebral cortex. These findings extend and complement recent *in vivo* MRI findings of Rosas and colleagues (2008) showing that variable patterns of cortical thinning in patients with Huntington's disease parallels clinical heterogeneity. The mechanisms underlying neuronal loss in the cerebral cortex are still unclear but may be a combination of disrupted microcircuitry, excitotoxicity and neurochemical imbalances. The cortical degeneration-to-symptom relationship we report here suggests that cortical neurodegeneration is a key component in understanding the neural basis of clinical hereogeneity in Huntington's disease.

Acknowledgements

We express our appreciation to the Huntington's families in New Zealand and the Huntington's Disease Associations of New Zealand for their generous and invaluable assistance, and to the Neurological Foundation of New Zealand Human Brain Bank.

Funding

Health Research Council of New Zealand; the Neurological Foundation of New Zealand; Matthew Oswin Memorial Trust.

References

Alexopoulos GS, Gunning-Dixon FM, Latoussakis V, Kanellopoulos D, Murphy CF. Anterior cingulate dysfunction in geriatric depression. Int J Geriatr Psychiatry 2008; 23: 347–55.

Altar CA, Cai N, Bliven T, Juhasz M, Conner JM, Acheson AL, et al. Anterograde transport of brain-derived neurotrophic factor and its role in the brain. Nature 1997; 389: 856–60.

Andre VM, Cepeda C, Venegas A, Gomez Y, Levine MS. Altered cortical glutamate receptor function in the R6/2 model of Huntington's disease. J Neurophysiol 2006; 95: 2108–19.

Augood SJ, Faull RLM, Love DR, Emson PC. Reduction in enkaphalin and substance P messenger RNA in the striatum of early grade Huntington's disease: a detailed cellular in situ hybridisation study. Neuroscience 1996; 72: 1023–36.

Brandt J, Butters N. The neuropsychology of Huntington's disease. Trends Neurosci 1986; 9: 118–20.

Cattaneo E, Rigamonti D, Goffredo D, Zuccato C, Squitieri F, Sipione S. Loss of normal huntingtin function: new developments in Huntington's disease research. Trends Neurosci 2001; 24: 182–8.

Cepeda C, Wu N, André VM, Cummings DM, Levine MS. The corticostriatal pathway in Huntington's disease. Prog Neurobiol 2007; 81: 253–71.

Claes S, Van Zand K, Legius E, Dom R, Malfroid M, Baro F, et al. Correlations between triplet repeat expansion and clinical features in Huntington's disease. Arch Neurol 1995; 52: 749–53.

Cudkowicz M, Kowall NW. Degeneration of pyramidal projection neurons in Huntington's disease cortex. Ann Neurol 1990; 27: 200–4.

Cummings DM, Andre VM, Uzgil BO, Gee SM, Fisher YE, Cepeda C, et al. Alterations in cortical excitation and inhibition in genetic mouse models of Huntington's disease. J Neurosci 2009; 29: 10371–86.

Davidson RJ, Pizzagalli D, Nitschke JB, Putnam K. Depression: perspective from affective neuroscience. Annu Rev Psychol 2002; 53: 545–74.

de la Monte SM, Vonsattel JP, Richardson EP Jr. Morphometric demonstration of atrophic changes in the cerebral cortex, white matter, and neostriatum in Huntington's disease. J Neuropathol Exp Neurol 1988; 47: 516–25.

Deng YP, Albin RL, Penney JB, Young AB, Anderson KD, Reiner A. Differential loss of striatal projection systems in Huntington's disease: a quantitative immunohistochemical study. J Chem Neuroanat 2004; 27: 143–64.

DiProspero NA, Chen EY, Charles V, Plomann M, Kordower JH, Tagle DA. Early changes in Huntington's disease patient brains involve alterations in cytoskeletal and synaptic elements. J Neurocytol 2004; 33: 517–33.

Ebert D, Ebmeier KP. The role of the cingulate gyrus in depression: from functional anatomy to neurochemistry. Biol Psychiatry 1996; 39: 1044–50.

Eblen F, Graybiel AM. Highly restricted origin of prefrontal cortical inputs to striosomes in the macaque monkey. J Neurosci 1995; 15: 5999–6013.

Faull RL, Waldvogel HJ, Nicholson LF, Synek BJ. The distribution of GABAA-benzodiazepine receptors in the basal ganglia in Huntington's disease and in the quinolinic acid-lesioned rat. Prog Brain Res 1993; 99: 105–23.

Ferrante RJ, Kowall NW, Beal MF, Martin JB, Bird ED, Richardson EP Jr. Morphologic and histochemical characteristics of a spared subset of striatal neurons in Huntington's disease. J Neuropathol Exp Neurol 1987; 46: 12–27.

Ferrer I, Krupinski J, Goutan E, Marti E, Ambrosio S, Arenas E. Brain-derived neurotrophic factor reduces cortical cell death by ischemia after middle cerebral artery occlusion in the rat. Acta Neuropathol 2001; 101: 229–38.

Folstein S. Huntington's disease: a disorder of families. Baltimore, MD: Johns Hopkins University Press; 1989.

Gauthier LR, Charrin BC, Borrell-Pages M, Dompierre JP, Rangone H, Cordelieres FP, et al. Huntingtin controls neurotrophic support and survival of neurons by enhancing BDNF vesicular transport along microtubules. [See comment]. Cell 2004; 118: 127–38.

Georgiou-Karistianis N, Sritharan A, Farrow M, Cunnington R, Stout J, Bradshaw J, et al. Increased cortical recruitment in Huntington's disease using a Simon task. Neuropsychologia 2007; 45: 1791–800.

Georgiou N, Bradshaw JL, Chiu E, Tudor A, O'Gorman L, Phillips JG. Differential clinical and motor control function in a pair of monozygotic twins with Huntington's disease. Mov Disord 1999; 14: 320–5.

Glass M, van Dellen A, Blakemore C, Hannan AJ, Faull RL. Delayed onset of Huntington's disease in mice in an enriched environment correlates with delayed loss of cannabinoid CB1 receptors. Neuroscience 2004; 123: 207–12.

Gomez-Esteban JC, Lezcano E, Zarranz JJ, Velasco F, Garamendi I, Perez T, et al. Monozygotic twins suffering from Huntington's disease show different cognitive and behavioural symptoms. Eur Neurol 2007; 57: 26–30.

Gu X, Andre V, Cepeda C, Li S-H, Li X-J, Levine M, et al. Pathological cell-cell interactions are necessary for striatal pathogenesis in a conditional mouse model of Huntington's disease. Mol Neurodegener 2007; 2: 8.

Gu X, Li C, Wei W, Lo V, Gong S, Li S-H, et al. Pathological cell-cell interactions elicited by a neuropathogenic form of mutant Huntingtin contribute to cortical pathogenesis in HD mice. Neuron 2005; 46: 433–44.

Gundersen HJ, Jensen EB. The efficiency of systematic sampling in stereology and its prediction. J Microsc 1987; 147: 229–63.

Gundersen HJG, Jensen EBV, Kieu K, Nielsen J. The efficiency of systematic sampling in stereology - reconsidered. J Microsc 1999; 193: 199–211.

Gusella J. Huntington's disease. In: Harris H, Hirschhorn K, editors. Advances in human genetics. New York: Plenum Press; 1991. pp. 125–51.

Halliday GM, McRitchie DA, Macdonald V, Double KL, Trent RJ, McCusker E. Regional specificity of brain atrophy in Huntington's disease. Exp Neurol 1998; 154: 663–72.

Harrison PJ. The neuropathology of primary mood disorder. Brain 2002; 125: 1428–49.

Hedreen JC, Folstein SE. Early loss of neostriatal striosome neurons in Huntington's disease. J Neuropathol Exp Neurol 1995; 54: 105–20.

Hedreen JC, Peyser CE, Folstein SE, Ross CA. Neuronal loss in layers V and VI of cerebral cortex in Huntington's disease. Neurosci Lett 1991; 133: 257–61.

Heinsen H, Strik M, Bauer M, Luther K, Ulmar G, Gangnus D, et al. Cortical and striatal neurone number in Huntington's disease. Acta Neuropathol 1994; 88: 320–33.

Hodges A, Strand AD, Aragaki AK, Kuhn A, Sengstag T, Hughes G, et al. Regional and cellular gene expression changes in human Huntington's disease brain. Hum Mol Genet 2006; 15: 965–77.

Kim JS, Reading SA, Brashers-Krug T, Calhoun VD, Ross CA, Pearlson GD. Functional MRI study of a serial reaction time task in Huntington's disease. Psychiatry Res 2004; 131: 23–30.

Konarski JZ, McIntyre RS, Kennedy SH, Rafi-Tari S, Soczynska JK, Ketter TA. Volumetric neuroimaging investigations in mood disorders: bipolar disorder versus major depressive disorder. Bipolar Disord 2008; 10: 1–37.

Laforet GA, Sapp E, Chase K, McIntyre C, Boyce FM, Campbell M, et al. Changes in cortical and striatal neurons predict behavioral and electrophysiological abnormalities in a transgenic murine model of Huntington's disease. J Neurosci 2001; 21: 9112–23.

Macdonald V, Halliday G. Pyramidal cell loss in motor cortices in Huntington's disease. Neurobiol Dis 2002; 10: 378–86.

Macdonald V, Halliday GM, Trent RJ, McCusker EA. Significant loss of pyramidal neurons in the angular gyrus of patients with Huntington's disease. Neuropathol Appl Neurobiol 1997; 23: 492–5.

Mann DM, Oliver R, Snowden JS. The topographic distribution of brain atrophy in Huntington's disease and progressive supranuclear palsy. Acta Neuropathol 1993; 85: 553–9.

Morton AJ, Nicholson LFB, Faull RLM. Compartmental loss of NADPH diaphorase in the neuropil of the human striatum in Huntington's disease. Neuroscience 1993; 53: 159–68.

Myers RH, Vonsattel JP, Paskevich PA, Kiely DK, Stevens TJ, Cupples LA, et al. Decreased neuronal and increased oligodendroglial densities in Huntington's disease caudate nucleus. J Neuropathol Exp Neurol 1991; 50: 729–42.

Olsen JM, Penney JB, Shoulson I, Young AB. Inhomogeneities of striatal receptor binding in Huntington's disease. Neurology 1986; 36: 342.

Oorschot DE. Are you using neuronal densities, synaptic densities or neurochemical densities as your definitive data? There is a better way to go. Prog Neurobiol 1994; 44: 233–47.

Paulsen JS. Functional imaging in Huntington's disease. Exp Neurol 2009; 216: 272–77.

Penney JB, Vonsattel JP, MacDonald ME, Gusella JF, Myers RP. CAG repeat number governs the development rate of pathology in Huntington's disease. Ann Neurol 1997; 41: 689–92.

Reiner A, Albin RL, Anderson KD, D'Amato CJ, Penney JB, Young AB. Differential loss of striatal projection neurons in Huntington disease. Proc Natl Acad Sci USA 1988; 85: 5733–7.

Rosas HD, Feigin AS, Hersch SM. Using advances in neuroimaging to detect, understand, and monitor disease progression in Huntington's disease. NeuroRx 2004; 1: 263–72.

Rosas HD, Hevelone ND, Zaleta AK, Greve DN, Salat DH, Fischl B. Regional cortical thinning in preclinical Huntington disease and its relationship to cognition. Neurology 2005; 65: 745–7.

Rosas HD, Koroshetz WJ, Chen YI, Skeuse C, Vangel M, Cudkowicz ME, et al. Evidence for more widespread cerebral pathology in early HD: an MRI-based morphometric analysis. Neurology 2003; 60: 1615–20.

Rosas HD, Liu AK, Hersch S, Glessner M, Ferrante RJ, Salat DH, et al. Regional and progressive thinning of the cortical ribbon in Huntington's disease. Neurology 2002; 58: 695–701.

Rosas HD, Salat DH, Lee SY, Zaleta AK, Pappu V, Fischl B, et al. Cerebral cortex and the clinical expression of Huntington's disease: complexity and heterogeneity. Brain 2008; 131: 1057–68.

Sapp E, Schwarz C, Chase K, Bhide PG, Young AB, Penney JB, et al. Huntingtin localisation in brains of normal and Huntington's disease patients. Ann Neurol 1997; 42: 604–12.

Selemon LD, Rajkowska G, Goldman-Rakic PS. Evidence for progression in frontal cortical pathology in late-stage Huntington's disease. J Comp Neurol 2004; 468: 190–204.

Seto-Oshima A, Emson PC, Lawson E, Mountjoy CQ, Carrasco LH. Loss of matrix calcium-binding protein-containing neurons in Huntington's disease. Lancet 1988; 331: 1252–5.

Sotrel A, Paskevich PA, Kiely DK, Bird ED, Williams RS, Myers RH. Morphometric analysis of the prefrontal cortex in Huntington's disease. Neurology 1991; 41: 1117–23.

Sotrel A, Williams RS, Kaufmann WE, Myers RH. Evidence for neuronal degeneration and dendritic plasticity in cortical pyramidal neurons of Huntington's disease: a quantitative Golgi study. Neurology 1993; 43: 2088–96.

Spampanato J, Gu X, Yang XW, Mody I. Progressive synaptic pathology of motor cortical neurons in a BAC transgenic mouse model of Huntington's disease. Neuroscience 2008; 157: 606–20.

Spires TL, Grote HE, Varshney NK, Cordery PM, van Dellen A, Blakemore C, et al. Environmental enrichment rescues protein deficits in a mouse model of Huntington's disease, indicating a possible disease mechanism. J Neurosci 2004; 24: 2270–6.

Strand AD, Baquet ZC, Aragaki AK, Holmans P, Yang L, Cleren C, et al. Expression profiling of Huntington's disease models suggests that brain-derived neurotrophic factor depletion plays a major role in striatal degeneration. J Neurosci 2007; 27: 11758–68.

The Huntington's Disease Collaborative Research Group. A novel gene containing a trinucleotide repeat that is expanded and unstable on Huntington's disease chromosomes. Cell 1993; 72: 971–83.

Thiruvady DR, Georgiou-Karistianis N, Egan GF, Ray S, Sritharan A, Farrow M, et al. Functional connectivity of the prefrontal cortex in Huntington's disease. J Neurol Neurosurg Psychiatry 2007; 78: 127–33.

Thompson JC, Snowden JS, Craufurd D, Neary D. Behavior in Huntington's disease: dissociating cognition-based and mood-based changes. J Neuropsychiatry Clin Neurosci 2002; 14: 37–43.

Tippett LJ, Waldvogel HJ, Thomas SJ, Hogg VM, van Roon-Mom W, Synek BJ, et al. Striosomes and mood dysfunction in Huntington's disease. Brain 2007; 130: 206–21.

van Dellen A, Blakemore C, Deacon R, York D, Hannan AJ. Delaying the onset of Huntington's in mice. Nature 2000; 404: 721–2.

van Roon-Mom WMC, Hogg VM, Tippett LJ, Faull RLM. Aggregate distribution in frontal and motor cortex in Huntington's disease brain. Neuroreport 2006; 17: 667–70.

Vonsattel JP, DiFiglia M. Huntington disease. J Neuropathol Exp Neurol 1998; 57: 369–84.

Vonsattel JP, Myers RH, Stevens TJ, Ferrante RJ, Bird ED, Richardson EP Jr. Neuropathological classification of Huntington's disease. J Neuropathol Exp Neurol 1985; 44: 559–77.

Vonsattel JPG, Ge P, Kelly L. Huntington's disease. In: Esiri MM, Morris JH, editors. The neuropathology of dementia. Cambridge: Cambridge University Press; 1997. pp. 219–33.

Waldvogel HJ, Curtis MA, Baer K, Rees MI, Faull RLM. Immunohistochemical staining of post-mortem adult human brain sections. Nat Protoc 2006; 1: 2719–32.

West MJ, Gundersen HJ. Unbiased stereological estimation of the number of neurons in the human hippocampus. J Comp Neurol 1990; 296: 1–22.

Wexler NS, Lorimer J, Porter J, Gomez F, Moskowitz C, Shackell E, et al. Venezuelan kindreds reveal that genetic and environmental factors modulate Huntington's disease age of onset. Proc Natl Acad Sci USA 2004; 101: 3498–503.

Whitefield JE, Williams L, Snow K, Dixon J, Winship I, Stapleton PM, et al. Molecular analysis of the Huntington's disease gene in New Zealand. N Z Med J 1996; 109: 27–30.

Wolf RC, Sambataro F, Vasic N, Schonfeldt-Lecuona C, Ecker D, Landwehrmeyer B. Aberrant connectivity of lateral prefrontal networks in presymptomatic Huntington's disease. Exp Neurol 2008; 213: 137–44.

Zappacosta B, Monza D, Meoni C, Austoni L, Soliveri P, Gellera C, et al. Psychiatric symptoms do not correlate with cognitive decline, motor symptoms, or CAG repeat length in Huntington's disease. Arch Neurol 1996; 53: 493–97.

Zuccato C, Ciammola A, Rigamonti D, Leavitt BR, Goffredo D, Conti L, et al. Loss of huntingtin-mediated BDNF gene transcription in Huntington's disease. Science 2001; 293: 493–8.